Calculations of Premixed Turbulent Flames by PDF Methods

M. S. ANAND

Allison Gas Turbine Division, General Motors Corporation, Indianapolis, IN 46206

and

S. B. POPE

Sibley School of Mechanical and Aerospace Engineering, Cornell University, Ithaca, NY 14853

Idealized premixed turbulent flames are studied using probability density function (pdf) methods. A modeled transport equation for the joint pdf of velocity and the reaction progress variable is solved by a Monte Carlo method. Detailed calculations of flame properties and flow statistics, including the flame speed, the scalar flux, the turbulence intensities, the kinetic energy budget and conditional statistics are presented for different density ratios. Results are compared with the limited available experimental data and the calculations based on the Bray–Moss–Libby (BML) model. Compared to the BML model, the present pdf approach has several advantages: fewer processes have to be modeled, more information can be extracted from the solution, and the method is directly applicable to multidimensional flames.

INTRODUCTION

The aerothermochemistry of turbulent combustion—the complex interaction between several interconnected processes of reaction, diffusion, and volume expansion occurring in a turbulent flow field—is one of the less understood aspects of turbulent reacting flows [1]. Reaction is influenced by the turbulence, which in turn is significantly affected by the reaction and the accompanying volume expansion.

The present work is concerned with a class of turbulent reacting flows, namely, premixed turbulent flames. Idealized premixed turbulent flames are studied using probability density function (pdf) methods [2]. Premixed turbulent flames are important because of their occurrence in spark ignition engines [3, 4], jet engines with reheat, and in industry [5]. Premixed turbulent flames have been studied theoretically with some success using conventional turbulence models and approaches, prominent among which is the Bray–Moss–Libby (BML) model [6, 7]. The present work is a sequel to the pdf calculations of idealized constant-density premixed turbulent flames by Pope and Anand [8]. The latter work was concerned with the influence of the microscale structure of the flame on macroscale properties—the turbulent flame speed, for example. The present work is concerned with the effect of variable density on the macroscale properties of the flame.

The flame under consideration is an idealized premixed turbulent flame which is statistically stationary and one-dimensional, and propagates through high-Reynolds-number turbulence which is nondecaying, homogeneous, and isotropic upstream of the flame. The flame is studied with density ratio (R)—the ratio of the unburned gas

Published by Elsevier Science Publishing Co., Inc.
52 Vanderbilt Avenue, New York, NY 10017

0010-2180/87/$03.50

density to the burned gas density—as a parameter. A one-step reaction is assumed, adopting the Bray—Moss model for premixed flames [9], so that the instantaneous thermochemical state is uniquely related to a single scalar variable, the reaction progress variable $c(\mathbf{x}, t)$. (The progress variable is zero in the unburned reactants and unity in the burned products.) The theoretical approach used in the present study is distinctly different from conventional presumed-pdf approaches in that the form of the pdf of the scalar c is not assumed; rather the transport equation for the joint pdf of the velocities $\mathbf{V}(\mathbf{x}, t)$ and the progress variable $c(\mathbf{x}, t)$ is solved to obtain the joint pdf [2, 10]. This approach offers important advantages over conventional turbulence models for treating turbulent reacting flows since reaction and convection (by mean and fluctuating velocities) are treated exactly in the pdf transport equation and need not be modeled. The mean pressure gradient and the variable density also appear in closed form. In addition, the joint pdf contains a more complete representation of the flow field than its first few moments only. The terms in the pdf equation representing the effects of molecular transport and pressure fluctuations need to be modeled. We use, for these terms, models that have been developed and tested for turbulent shear flows [2, 11, 12]. The pdf transport equation is then solved using a Monte Carlo method [2, 10].

The flame properties calculated in the present study are the turbulent flame speed (S_T); the flame thickness (δ_T); the profiles of the mean and variance of the progress variable; and the profiles of mean velocity, scalar flux, mean pressure gradient, and turbulent intensities through the flame. The balance of the various terms in the streamwise turbulent intensity equation is studied to understand turbulence production in the flame. The conditional mean velocities and other statistics (conditioned on the fluid being unburned or burned) are also calculated.

The present approach has certain additional advantages over the BML approach. The turbulent flame speed and the structure of the flame (spatial variation of the mean of the progress variable) are determined as part of the solution in the present approach. In the BML theory, the flame speed is required as an input to the calculations and the spatial structure of the flame is not resolved without requiring additional modeling.

Experimental data for strictly one-dimensional premixed turbulent flames are unavailable since such flames are idealizations and difficult to realize in practice. Inasmuch as it considers simple flames, the present study is viewed as a first step to calculating more realizable flames like the V-flame, for which abundant experimental data exist. Following Bray et al. [6] and Libby [7], we compare our results with the limited experimental data of Moss [14] for a Bunsen flame interpreted to correspond to 1-D (one-dimensional) flames [6, 7] with the understanding that small errors and ambiguities in the interpretation can cause large uncertainties in the transformed data. The results from the present study are primarily compared with those from the BML theory [6, 7].

The next section describes the governing equations for the 1-D premixed turbulent flame and the modeling of the pdf transport equation. The modeling in the present study and the BML theory are compared in the third section. Results are reported for density ratios between 1 and 10 and discussed in the fourth section.

THEORY AND MODELING

The schematic diagram of an idealized 1-D premixed turbulent flame in steady state is shown in Fig. 1. All mean quantities are invariant with time in a coordinate system fixed to the flame. Further, all mean quantities vary only in one direction, the x-direction. The flow, as shown in Fig. 1, is along the x-direction, which is normal to the time-averaged flame sheet. However, the analysis is valid even for an "oblique" flame, i.e., when the flow makes an angle with the x-direction, as long as the flame is unconfined and the streamlines are unconstrained [7, 13].

In the idealized "normal" flame under consideration (Fig. 1), premixed reactants with density ρ_u flow into an infinite planar turbulent flame with mean velocity U_0, which is, by definition, the turbulent flame speed S_T. The turbulence in the incoming reactant stream is (by assumption) isotropic and nondecaying with turbulent kinetic

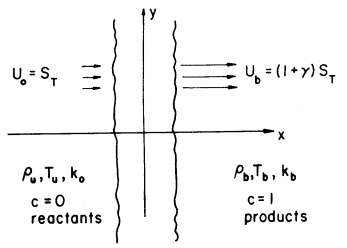

Fig. 1. Schematic diagram of a steady 1-D premixed turbulent flame. (Note: $1 + \gamma \equiv R \equiv \rho_u/\rho_b$.)

energy k_0 ($=3u_0'^2/2$, where u_0' is the upstream rms velocity fluctuation). The reactants are converted to products with accompanied heat release upon passage through the flame. The density falls and the resultant volume expansion causes the flow to accelerate. In the fully burned region downstream of the flame, the density is ρ_b, the mean velocity normal to the flame is U_b, and the turbulence is anisotropic with kinetic energy k_b.

The principal independent variables are position $\mathbf{x} \equiv (x_1, x_2, x_3) \equiv (x, y, z)$ and time t. The principal dependent variables are the progress variable $c(\mathbf{x}, t)$ and the velocity $\mathbf{U}(\mathbf{x}, t)$ with components $(U_1, U_2, U_3) \equiv (u, v, w)$.

In presenting the mean conservation and balance equations, we use Favre averages (density weighted averages) since their use greatly simplifies these equations for variable density flows [15]. A general variable q is decomposed into its (Favre) mean $\tilde{q}$ and fluctuation q'':

$$q = \langle \rho q \rangle / \langle \rho \rangle + q'' = \tilde{q} + q'', \tag{1}$$

where $\langle\ \rangle$ indicates the conventional mean. It should be noted that while the Favre mean of q'' is zero ($\widetilde{q''} = 0$), the conventional mean is generally not ($\langle q'' \rangle \neq 0$). Mostly, the Favre decomposition is used for all quantities except pressure p, which is decomposed into its conventional mean $\langle p \rangle$ and fluctuation p'.

The conservation equations (unaveraged) for mass and j-direction momentum are

$$\frac{\partial \rho}{\partial t} + \frac{\partial}{\partial x_i}(\rho U_i) = 0 \tag{2}$$

and

$$\frac{\partial}{\partial t}(\rho U_j) + \frac{\partial}{\partial x_i}(\rho U_i U_j) = -\frac{\partial p}{\partial x_j} + \frac{\partial \tau_{ij}}{\partial x_i} + \frac{1}{2}\rho u_j'' \frac{\epsilon}{k}, \tag{3}$$

where k is the turbulent kinetic energy, ϵ is the rate of viscous dissipation of k, and τ_{ij} is the sum of the viscous and viscous–diffusive stress tensors. The precise form of τ_{ij} is inconsequential in the present study (as well as BML theory) since its effects are modeled. The last term in Eq. (3) represents a source of kinetic energy that exactly balances the energy loss due to viscous dissipation. ($\mathbf{u}''$ rather than $\mathbf{U}''$ is used for fluctuating velocity.) This term is nonphysical and has been added to keep the turbulence from decaying due to viscous dissipation. It can be shown [13] that, in the idealized situation considered here, the flame is unstable in decaying upstream turbulence. (If a flame stabilized in decaying turbulence, say in grid-generated turbulence, is perturbed by a displacement toward the grid, the flame encounters a level of turbulence greater than at its previous location, which causes an increase in the flame speed and further acceleration of the flame toward the grid. In the idealized situation considered here, this process will continue until the flame finally collides with the grid. In practice, the flame may be stabilized near the grid as a result of heat loss to the surroundings. A similar analysis shows that if the flame is displaced away from the grid, the flame speed decreases continuously, resulting in the blow-off of the flame. From the above consideration it can be seen that the flame is neutrally stable in nondecaying upstream turbulence. The inclusion of the last term in Eq. (3) is consistent with the assumption of no viscous dissipation outside the flame, made in the BML model [6, 7]. The term has no contribution to the mean momentum equation, and the contributions due to viscous dissipation to the kinetic energy and the scalar flux budgets within the flame are small in comparison to the other terms in the budgets, as seen from the results of Bray et al. [6].) The ratio k/ϵ is taken to be the characteristic turbulent time scale (τ), where k is given by $\widetilde{u_i'' u_i''}/2$ (with

implied sum over all three components for repeated indices).

The conservation equation for the scalar $c(\mathbf{x}, t)$ is

$$\frac{\partial}{\partial t}(\rho c)+\frac{\partial}{\partial x_i}(\rho U_i c)=-\frac{\partial J_i}{\partial x_i}+\rho S(c), \tag{4}$$

where J_i is the diffusive mass flux of c due to molecular transport and $S(c)$ is the rate of change of c due to reaction and is taken to be

$$S(c)=S^*(c)/\tau_R, \tag{5}$$

where τ_R is the reaction time scale. As in the previous work [8] the normalized reaction rate $S^*(c)$ is taken to be the Arrehenius expression

$$S^*(c)=6.11\times 10^7 c(1-c) \times \exp[-30{,}000/(300+1800c)], \tag{6}$$

which corresponds to an activation temperature of 30,000K and unburned and fully burned temperatures of 300K and 1800K, respectively. Again, the precise form of J_i is not considered since molecular transport is modeled in the present study as well as in the BML theory.

The joint pdf $f(\mathbf{V}, C; \mathbf{x}, t)$ [or $f(\mathbf{V}, C)$ to be brief] is defined to be the probability density at a given $\mathbf{x}$ and t of the simultaneous events $\mathbf{U}(\mathbf{x}, t) = \mathbf{V}$ and $c(\mathbf{x}, t) = C$, where $\mathbf{V}$ and C are independent velocity and composition variables. As written, the pdf $f(\mathbf{V}, C)$ is a function of eight independent variables—three velocity variables V_1, V_2, V_3, the composition variable C, three spatial variables, and time. But, for the statistically one-dimensional and stationary flame under consideration, three independent variables can be eliminated so that

$$f(V, C; x, t)=f(V, C; x). \tag{7}$$

For variable-density flows it is more natural to consider the mass density function (mdf) rather than the pdf [2]. The mdf (F), simplified for a statistically 1-D case, is defined by

$$F(V, C, x; t)=\rho(C)f(V, C; x, t). \tag{8}$$

The mean of any quantity $Q(\mathbf{U}, c)$ can be evaluated from the following integral over the velocity-composition ($\mathbf{V}$–C) space:

$$\langle\rho\rangle\tilde{Q}(U, c)=\int\int Q(V, C) \times F(V, C, x; t)\, dV\, dC. \tag{9}$$

The exact evolution equation for the pdf (rather the mdf) can be derived from Eqs. (2)–(4) using methods described in [2, 10]:

$$\frac{\partial F}{\partial t}+V_i\frac{\partial F}{\partial x_i}-\frac{1}{\rho(C)}\frac{\partial\langle p\rangle}{\partial x_i}\frac{\partial F}{\partial V_i} +\frac{\partial}{\partial C}[S(C)F]+\frac{1}{2\tau}\frac{\partial}{\partial V_i}(FV_i) =-\frac{\partial}{\partial V_j}[\langle A_j(x, t)|V, C\rangle F] -\frac{\partial}{\partial C}[\langle\Theta(x, t)|V, C\rangle F], \tag{10}$$

where

$$\rho A_j(x, t)=\frac{\partial\tau_{ij}}{\partial x_i}-\frac{\partial p'}{\partial x_j}$$

and

$$\rho\Theta(x, t)=-\frac{\partial J_i}{\partial x_i}.$$

[For any quantity Q, $\langle Q|\mathbf{V}, C\rangle$ denotes the expectation conditional upon the event $\mathbf{U}(\mathbf{x}, t) = \mathbf{V}$ and $c(\mathbf{x}, t) = C$.] The terms on the left-hand side of Eq. (10) are exact—ρ and S are known functions in C-space and the gradient of $\langle p\rangle$ can be determined from the mdf (see next section). The terms represent, respectively, the change in F with time, transport in physical space (convection), transport in velocity space by the mean pressure gradient, transport in composition space by reaction, and the addition of turbulent kinetic energy. All the above processes are thereby treated without approximation. The terms on the right-hand side of Eq. (10) contain, as unknowns, conditional expectations that have to be modeled.

Before discussing the modeling, certain flow parameters and related assumptions about the flow are discussed. The flow conditions upstream of the flame were described earlier in this section. The characteristic scales of turbulence in the upstream flow are the time scale $\tau \equiv k/\epsilon$, the velocity scale

u_0', and the length scale $l_0 \equiv u_0'\tau$, (The time scale τ is assumed constant through the flame. Justification for this assumption comes from the tentative results of the study by Bray et al. [16] which show that τ is constant through the flame.) The characteristic time scale for reaction is τ_R. From these scales and from the kinematic viscosity ν, two dimensionless parameters can be formed. We take these to be the (turbulent) Reynolds number $\mathrm{Re} \equiv u_0' l_0/\nu$ and the Damkohler number $\mathrm{Da} \equiv \tau/\tau_R$. Another important parameter is the density ratio $R(=\rho_u/\rho_b)$. For practical flames, R lies in the range 5–10. Density ratios between 1 and 10 are investigated in the present study. The Reynolds number is assumed to be arbitrarily large, so that models developed for high Reynolds number can be applied. According to the modeled equations, the exact value of Re does not affect the results except to determine the type of combustion. The Damkohler number, in conjunction with the Reynolds number, determines the type of combustion and hence the modeling used [8].

The modeling of the molecular diffusion term is influenced by the type of combustion [8]. Different regimes of premixed turbulent combustion—in particular, the extreme regimes of flamelet and distributed combustion—are discussed in Refs. [8] and [13]. Flamelet combustion, in which combustion occurs in thin sheets which locally have the properties of undisturbed laminar flames, occurs when $\mathrm{Re}^{1/2} \ll \mathrm{Da} \ll \mathrm{Re}$ (i.e., when $\delta_l \ll \eta_0$, where δ_l is the laminar flame thickness and η_0 is the upstream Kolmogorov length scale). Distributed combustion, in which reaction is distributed more uniformly in space and is not necessarily accompanied by steep gradients of c, occurs when $\mathrm{Da} \ll \mathrm{Re}^{1/2}$ (i.e., when $\eta_0 \ll \delta_l$). In the present study, only the flamelet regime is considered since there is some experimental evidence to suggest that combustion in practical flames is closer to the flamelet regime than to the distributed regime (e.g., [17]). In the case of flamelet combustion, the modeling is such [8] that the molecular diffusion term in Eq. (10), involving the conditional expectation of Θ, is modeled by the stochastic mixing model [11] while the reaction rate $S(C)$ is replaced by an effective rate $h(C)$ derived from the structure of a laminar flame [13]. (It should be noted that $h(C)$ *exactly* accounts for contributions from both $S(C)$ *and* Θ within the bulk of the laminar flamelet. The mixing model, whose contribution is negligible in the bulk of the flamelet, is required only to account for the effect of molecular diffusion at the edges (near $c = 0$ and $c = 1$). For large Damkohler numbers, it is seen [8] that $h(C)$ is large enough so that once the fluid attains (by turbulent mixing) a value of c greater than zero (of the order 1/Da), reaction proceeds rapidly, and a value close to $c = 1$ is reached almost instantaneously. This behavior, which corresponds to the asymptote $\mathrm{Da} \to \infty$, is approached even at moderate Damkohler numbers ($\mathrm{Da} > 20$). The resulting pdf of c, $f_c(C)$, is a double-delta function distribution with delta functions of strengths $\tilde{c}$ at $C = 1$ and $(1 - \tilde{c})$ at $C = 0$. The resulting variance of the scalar $\widetilde{(c'')^2}$ is $\tilde{c}(1 - \tilde{c})$. In the present study, the Damkohler number is assumed to be arbitrarily large, which is consistent with the assumption of fast chemistry in the BML theory. (Calculations with finite Da can be performed with the present approach [8, 13]. Also, distributed combustion can be computed by just retaining $S(C)$ instead of replacing it by $h(C)$ [8, 13].)

The effects of viscous dissipation [due to τ_{ij} in Eq. (10)] are modeled using the improved stochastic mixing model [11] for the velocities. The effect of the fluctuating pressure gradient [due to gradient of p' in Eq. (10)] is modeled by the stochastic reorientation model [2, 12]. The combined effect of the stochastic models on the Reynolds stresses is equivalent to that of Rotta's return-to-isotropy model [18], which is an acceptable model for constant-density flows. (The effect of the mixing model is dissipative, while the reorientation model redistributes energy among the various components.) In constant-density flows without mean velocity gradients, the fluctuating pressure field is solely due to turbulence and is termed "slow" pressure. Additional sources of pressure fluctuations arise in variable-density flows due to density gradients, velocity gradients, the velocity divergence, and the viscous shear stresses. These terms may be important and may have significant influence on quantities such as the turbulence kinetic energy, scalar flux, etc., though there is a lack of

evidence to draw firm conclusions. Usually, the effects of the fluctuating pressure gradient are neglected, as in the BML theory [6, 7], with the expectation that the effects of the mean pressure gradient are dominant. In the present study, however, only the effects of the "slow" pressure (due to turbulence alone) are considered by the stochastic reorientation model, and the additional effects are neglected.

Starting from an almost arbitrary initial condition, the modeled mdf equation is solved by a Monte Carlo method until steady state is reached [this is the reason for which the time rate of change term in Eq. (10) is retained]. The details of the modeling and the Monte Carlo method can be found in Ref. [13].

COMPARISON WITH THE BML MODELING

The set of conservation and balance equations used in the BML theory are the mean continuity, x-momentum and scalar equations, and the equations for $\widetilde{u''^2}$ ($\equiv \widetilde{u_1''^2}$) and $\widetilde{u''c''}$. First, the effect of the modeling in the present study on these equations is discussed. The modeling of these equations in the BML theory is then discussed and compared with that in the present study.

The modeling in the present study does not directly affect the mean conservation equations at steady-state, derived from Eqs. (2)–(4) with the assumption of high Reynolds number. They are

$$\frac{d}{dx}(\langle\rho\rangle\tilde{u}) = 0, \tag{11}$$

$$\frac{d}{dx}[\langle\rho\rangle(\tilde{u}^2 + \widetilde{u''^2})] = -\frac{d\langle p\rangle}{dx}, \tag{12}$$

$$\frac{d}{dx}[\langle\rho\rangle(\tilde{u}\tilde{c} + \widetilde{u''c''})] = \langle\rho\rangle\widetilde{S(c)}. \tag{13}$$

The mean continuity equation [Eq. (11)] implies that $\langle\rho\rangle\tilde{u}$ is a constant through the flame and, by definition, the constant is equal to $\rho_u S_T$:

$$\langle\rho\rangle\tilde{u} = \text{constant} \equiv \rho_u S_T. \tag{14}$$

A consequence of the single scalar formulation is that the density is uniquely calculated from the reaction progress variable:

$$\rho = \rho_u/(1+\gamma c) \quad \text{and} \quad \langle\rho\rangle = \rho_u/(1+\gamma\tilde{c}), \tag{15}$$

where $\gamma \equiv R - 1$. (The quantity γ is denoted by τ and is referred to as the heat release parameter in the BML studies.) From Eqs. (14) and (15) it can be seen that the mean streamwise velocity ($\tilde{u}$) is related to the mean progress variable ($\tilde{c}$) by the following relationship:

$$\tilde{u} = (\rho_u/\langle\rho\rangle)S_T = (1+\gamma\tilde{c})S_T. \tag{16}$$

[Note: $U_b = RU_0 = RS_T$ from Eq. (16).]

The equation for the mean pressure gradient then becomes [see Eq. (12)]

$$\frac{d\langle p\rangle}{dx} = -\frac{d}{dx}(\langle\rho\rangle\widetilde{u''^2}) - \gamma\rho_u S_T^2\frac{d\tilde{c}}{dx}. \tag{17}$$

The right-hand side of Eq. (17) is known from the mdf and the flame speed calculated in the Monte Carlo method [13]. Thus, the mean pressure gradient is a known quantity during the computations.

The effect of the modeling is apparent in the balance equations for $\widetilde{u''^2}$ and $\widetilde{u''c''}$. The modeled equations for these quantities, which can be derived from Eq. (10) using methods described in Ref. [2], are

$$\begin{aligned}\langle\rho\rangle\tilde{u}\frac{d\widetilde{u''^2}}{dx} + \frac{d}{dx}\langle\rho\rangle\widetilde{u''^3} + 2\langle\rho\rangle\widetilde{u''^2}\frac{d\tilde{u}}{dx} \\ + 2\langle u''\rangle\frac{d\langle p\rangle}{dx} - \langle\rho\rangle\frac{\widetilde{u''^2}}{\tau} \\ = -\langle\rho\rangle C_R'(\widetilde{u''^2} - 2k/3)/\tau - \langle\rho\rangle C_u\widetilde{u''^2}/\tau,\end{aligned} \tag{18}$$

$$\begin{aligned}\langle\rho\rangle\tilde{u}\frac{d}{dx}\widetilde{u''c''} + \frac{d}{dx}\langle\rho\rangle\widetilde{c''u''^2} + \langle\rho\rangle\widetilde{u''c''}\frac{d\tilde{u}}{dx} \\ + \langle\rho\rangle\widetilde{u''^2}\frac{d\tilde{c}}{dx} + \langle c''\rangle\frac{d\langle p\rangle}{dx} - \langle\rho\rangle\widetilde{u''S(c)} \\ - \langle\rho\rangle\widetilde{u''c''}/2\tau \\ = -\langle\rho\rangle C_f\widetilde{u''c''}/\tau.\end{aligned} \tag{19}$$

All the terms on the left-hand side in Eqs. (18) and (19) are exact, and the terms on the right-hand side are modeled. The terms on the right-hand side in Eq. (18) are due, respectively, to the stochastic reorientation and mixing models for the velocities. The term on the right-hand side of Eq. (19) is due to the combined effect of the stochastic models for the velocities and the scalar c. By definition, the value of C_u is equal to unity. With $C_u = 1$, the last terms on the left- and right-hand sides cancel each other in Eq. (18). The model constant C_R' is related to the Rotta constant C_R [18] by $C_R' = C_R - 1$, and the value $C_R = 1.5$ suggested by Launder et al. [19] is used in the present study. Following previous studies [8, 20], a value $C_f = 3.1$ is used. The quantities $\langle u'' \rangle$ and $\langle c'' \rangle$ in Eqs. (18) and (19) are known in terms of $\widetilde{c''^2}$ and $\widetilde{u''c''}$ from the definition of the Favre averages and from Eq. (15):

$$\langle u'' \rangle = \gamma \widetilde{u''c''}/(1+\gamma\tilde{c}) \quad \text{and} \quad \langle c'' \rangle = \gamma \widetilde{c''^2}/(1+\gamma\tilde{c}). \tag{20}$$

The following points of comparison can be made between the modeling in the present study and that in the BML theory [6, 7]:

1. The molecular (dissipation) effects [terms corresponding to those involving C_u and C_f in Eqs. (18) and (19)] are modeled in both studies.
2. The effects of fluctuating pressure are entirely neglected in the BML theory. The effects of "slow" pressure are accounted for in the present study.
3. In the BML theory, the variances of the transverse velocity fluctuations ($\widetilde{v''^2}$ and $\widetilde{w''^2}$) are assumed to be constant across the flame, while their variation across the flame, due to redistribution of k by "slow" pressure, is calculated in the present study.
4. All terms on the left-hand sides of Eqs. (18) and (19) are not known in the BML theory. The unconditional quantities in Eqs. (18) and (19)—mean velocity $\tilde{u}$ and correlations involving u'' and c''—can be expressed in terms of "conditional" quantities under the assumption of a double-delta function pdf of c. The expressions are listed in Refs. [7] and [13]. For example,

$$\widetilde{u''c''} = \tilde{c}(1-\tilde{c})(\langle u \rangle_b - \langle u \rangle_u), \tag{21}$$

$$\widetilde{u''^3} = (1-\tilde{c})[(\langle u \rangle_u - \tilde{u})^3 + 3(\langle u \rangle_u - \tilde{u})\langle u'^2 \rangle_u + \langle u'^3 \rangle_u] + \tilde{c}[(\langle u \rangle_b - \tilde{u})^3 + 3(\langle u \rangle_b - \tilde{u})\langle u'^2 \rangle_b + \langle u'^3 \rangle_b], \tag{22}$$

where $\langle\ \rangle_b$ and $\langle\ \rangle_u$ denote means conditional upon the fluid being burned ($c = 1$) or unburned ($c = 0$), respectively. The conditional fluctuations—for example, in $\langle u'^2 \rangle_b$—are departures from the conditional means (not from the unconditional means). In the BML theory, the unknown correlations are expressed in terms of the conditional quantities shown in Eqs. (21) and (22). Closure is then effected by modeling the following quantities.

   a) The term $\widetilde{u''S}$ is modeled. The sensitivity of the results to this modeling is not clear. But the modeling is expected to be crucial. The term $\widetilde{u''S}$ appears in closed form in the present study and need not be modeled.
   b) A model for the difference $(\langle u'^2 \rangle_b - \langle u'^2 \rangle_u)$ is required in the BML theory while all the conditional quantities are calculated in the present study. Therefore, the model used in the BML theory can be checked against the results of the present study.
   c) The conditional third moments $\langle u'^3 \rangle_u$ and $\langle u'^3 \rangle_b$ are assumed to be zero in the BML theory. The assumption can be checked since those quantities are calculated in the present study.

5. The closure noted above is effected by considering $\tilde{c}$ as the independent variable instead of x. A solution of the flame in terms of the physical space coordinate (x) is not possible with the BML theory without an additional model for $\tilde{S}$, while the structure of the flame is resolved in physical space in the present study.
6. An important feature of the present study is that the flame speed S_T is determined as part of the solution. A value for S_T has to be assumed in the BML theory.

Thus it is seen that many more quantities are modeled in the BML theory in addition to the quantities modeled in the present study. At the same time, the solution of the pdf yields more information about the flow than can be extracted from the BML theory.

RESULTS AND DISCUSSION

The turbulent flame speed (S_T) normalized by the upstream velocity variance (u_0') is shown in Fig. 2 as a function of the density ratio (R). The flame speed has a value $2.1u_0'$ for $R = 1.0$ and quickly drops, as R increases, to an asymptotic value of approximately $1.5u_0'$ by $R = 4.0$. This asymptotic value coincides exactly with the recent prediction of Gosman [21], in an extension to the study by Gosman and Hackberg [22], based on an earlier version of the BML theory. The value also falls well within the scatter of experimental data on flame speeds in the literature [7, 13]. It should be noted that Libby [7] and Bray et al. [6] assume a value of $S_T = 2.1u_0'$ for their calculations and a value $S_T = 2.5u_0'$ in order to compare their theory with the experiments of Moss [14].

The turbulent flame thickness (δ_T) normalized by the upstream length scale (l_0) is shown in Fig. 3 as a function of R. The thickness can be defined in many ways; for reasons of computational stability, we choose to define δ_T to be the standard deviation of the distribution

$$Z(x) \equiv \tilde{c}(1-\tilde{c}) \Big/ \int_{-\infty}^{\infty} \tilde{c}(1-\tilde{c})\, dx. \qquad (23)$$

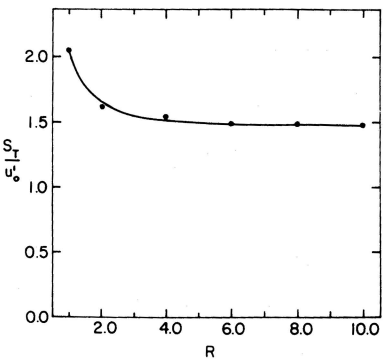

Fig. 2. Normalized turbulent flame speed against density ratio.

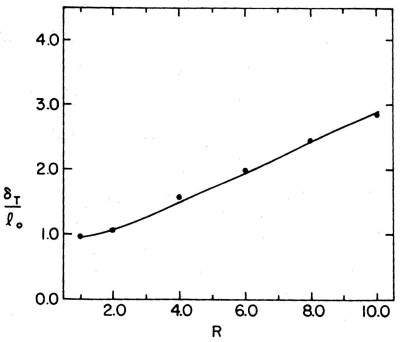

Fig. 3. Normalized turbulent flame thickness against density ratio.

The flame thickness is approximately equal to l_0 for the constant-density case ($R = 1.0$) and increases continually as R increases. The increase is linear with R beyond $R = 4.0$. The turbulent flame thickness is known to be of the order of the upstream turbulent length scale (l_0) [23]. The variation of δ_T with R is further discussed below.

Figure 4 shows the profile of the mean progress variable ($\tilde{c}$) as a function of the normalized spatial coordinate—normalized by the turbulent flame thickness—for all density ratios studied (the choice of origin for x is immaterial). The mean progress variable increases monotonically with x. It is surprising that in spite of the many nonlinear processes occurring in the flame, the structure of the flame in a coordinate system nondimensiona-

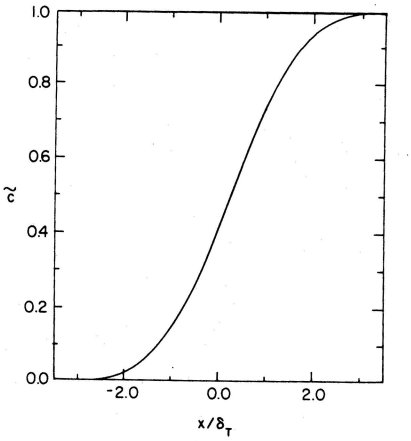

Fig. 4. Mean progress variable against distance normalized by turbulent flame thickness. The profile is universal for all density ratios.

lized by the flame thickness adopts a universal profile for all density ratios, including the constant-density case. It can be shown [13] that this fact combined with the linear increase of δ_T with R implies that the mass of fluid contained within the flame is approximately the same for all density ratios. The effect of the larger heat release (i.e., larger R) is to increase proportionately the volume occupied by the same mass within the flame. It is perhaps possible to rescale the governing equations for the flame to show that this is indeed true, but such a task is not undertaken here. It should be noted that the actual extent of the flame (over which $\tilde{c}$ varies substantially) is nearly six times the mathematically defined thickness (δ_T) of the flame (see Fig. 4). The computed values of $\widetilde{c''^2}$ were, inevitably, in excellent agreement with the theoretically expected values $[\tilde{c}(1 - \tilde{c})]$ for flamelet combustion.

The mean streamwise velocities computed from the mdf [Eq. (9)] were also in agreement with the expected values from Eq. (16). The conditional burned and unburned mean streamwise velocities normalized by S_T are presented in Fig. 5 as functions of $\tilde{c}$. The results from the present study ($R = 8.0$, Fig. 5a) and those from the BML theory [6, 7] and Moss's experiments [14] ($R = 7.5$, Fig. 5b) are presented. [Since $\tilde{c}$ is a monotonic function of x (Fig. 4), profiles through the flame can be plotted as functions of $\tilde{c}$ instead of x. Variations of quantities with respect to x can still be deduced from Fig. 4.] Figure 5a shows that the value of $\langle u \rangle_b$ at $\tilde{c} = 1$ is equal to RS_T, as expected [see note following (Eq. 16)], and the value of $\langle u \rangle_u$ at $\tilde{c} = 0$ is equal to S_T. The burned mean velocity is greater than the unburned mean velocity nearly everywhere within the flame. This is due to the effect of the mean pressure gradient accelerating the burned fluid more (by a factor of the density ratio) than the unburned fluid. The observed phenomenon of countergradient diffusion [24] (that is to say that the scalar flux $\widetilde{u''c''}$ is of the same sign as the gradient of $\tilde{c}$, in contradiction to gradient transport) is a manifestation of this relative motion between the burned and unburned fluid [see Eq. (21)]. [In the present context, a positive value of $(\langle u \rangle_b - \langle u \rangle_u)$ indicates countergradient diffusion, and a negative value indicates

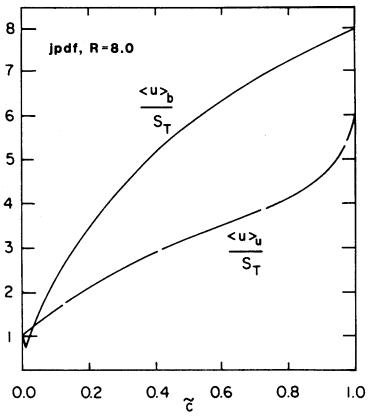

Fig. 5a.

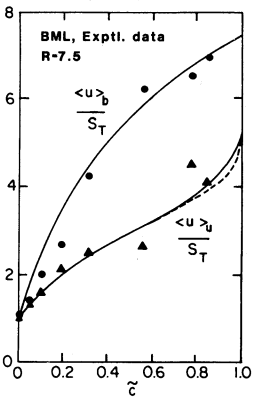

Fig. 5b.

Fig. 5. Conditional velocities normalized by flame speed against mean progress variable: (a) present study, $R = 8.0$; (b) BML theory and experimental data $R = 7.5$ (solid line, Libby [7]; dotted line, Bray et al. [6]; symbols, data from Moss [14]).

gradient diffusion.] A small region of gradient diffusion near the cold boundary (near $\tilde{c} = 0$) is indicated in Fig. 5a, which is necessary for flame holding and stability [7]. The present results (Fig. 5a) are in good agreement with the results of the BML theory and the experimental data of Moss (Fig. 5b) both qualitatively and quantitatively (note the slight difference in density ratios for Figs. 5a and 5b).

The mean pressure gradient (normalized by $\rho_u u_0'^2/l_0$) is shown in Fig. 6 against $\tilde{c}$ for all density ratios studied. It is seen that for $R > 1$, the mean pressure gradient is negative nearly everywhere within the flame, indicating that the mean

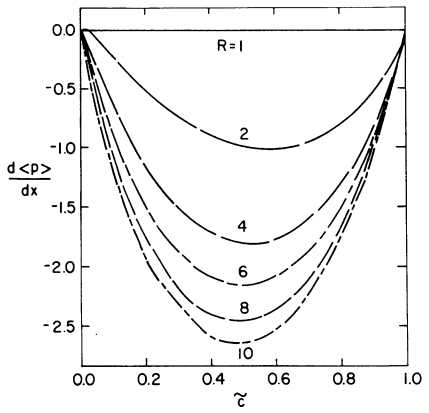

Fig. 6. Mean pressure gradient normalized by $\rho_u u_0'^2/l_0$ against mean progress variable with density ratio as a parameter.

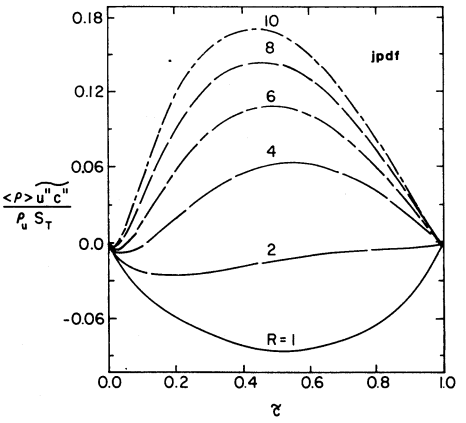

Fig. 7a.

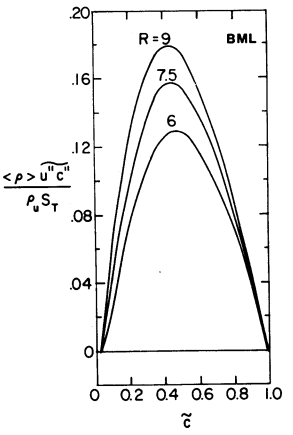

Fig. 7b.

Fig. 7. Mean mass flux of progress variable normalized by the total mean mass flux of fluid against mean progress variable for different density ratios: (a) present study; (b) BML theory (Bray et al. [6]).

pressure decreases through the flame. The mean pressure is constant for $R = 1$. The absolute value of the mean pressure gradient, which reaches a maximum near $\tilde{c} = 0.5$, increases with increasing R (Fig. 6).

The mean turbulent mass flux of the progress variable in the streamwise direction ($\langle\rho\rangle\widetilde{u''c''}$) is shown as a fraction of the mean mass flow through the flame ($\rho_u S_T$) against $\tilde{c}$ for different density ratios in Fig. 7. The results from the present study are shown in Fig. 7a, and those from the BML theory [6] are shown in Fig. 7b. Figure 7b shows that the scalar flux is positive almost everywhere within the flame for $R \geq 4$, indicating countergradient diffusion. For $R = 1$ and $R = 2$, the flux is negative everywhere, which supports the gradient diffusion assumption by conventional turbulence models for nearly-constant-density flows. The explanations for the above trends lie in the balance equation for the scalar flux [Eq. (19)]. An inspection of the terms in Eq. (19) reveals that the term due to the mean pressure gradient ($\langle c''\rangle\, d\langle p\rangle/dx$) is a production term and the terms due to the mean velocity gradient ($\langle\rho\rangle\widetilde{u''c''}\, d\tilde{u}/dx$) and the gradient of $\tilde{c}$ ($\langle\rho\rangle\widetilde{u''^2}\, d\tilde{c}/dx$) are destruction terms. It can be deduced from Eq. (16) and Figs. 3 and 4 that $d\tilde{u}/dx$ remains nearly constant with respect to R, while $d\tilde{c}/dx$ varies inversely and $d\langle p\rangle/dx$ increases with R (Fig. 6). Thus at low density ratios, the destruction terms are dominant (especially the one due to the gradient of $\tilde{c}$) and cause a negative scalar flux, but at higher density ratios the pressure gradient term dominates, causing a positive scalar flux.

The results for the scalar flux from the present study (Fig. 7a) are compared with those from the BML theory [6] (Fig. 7b). The results are in good qualitative and quantitative agreement. The peak values of the scalar flux occur at the same values of $\tilde{c}$ in both the studies for the range of density ratios compared, though the peak values are slightly higher in the BML results than in the present study for corresponding density ratios. Based on the sensitivity analysis (to the value of

S_T) performed by Libby [7] and the discussion by Anand [13], the difference can be attributed to the higher value of $S_T(=2.1u_0')$ chosen in the BML theory compared to the calculated value $(=1.5u_0')$ in the present study even though the flux is normalized by $\rho_u S_T$ in Fig. 7. The results from both the present study and the BML study (Figs. 7a and 7b) show the region of gradient diffusion (negative scalar flux) near $\tilde{c} = 0$, though the extent is slightly larger (up to $\tilde{c} = 0.05$ for $R = 6$) in the present study than in the BML study (up to $\tilde{c} = 0.03$ for $R = 6$).

We now investigate the effect and importance of the various terms in the model equation for the streamwise velocity variance $\widetilde{u''^2}$ (rather than for the turbulent kinetic energy, since $\widetilde{v''^2}$ and $\widetilde{w''^2}$ vary only slightly through the flame). Equation (18) can be rewritten (with $C_u = 1.0$) as follows:

$$\text{Rem.} = -\langle\rho\rangle\tilde{u}\frac{d\widetilde{u''^2}}{dx} - \frac{d}{dx}\langle\rho\rangle\widetilde{u''^3} - 2\langle\rho\rangle\widetilde{u''^2}\frac{d\tilde{u}}{dx} - 2\langle u''\rangle\frac{d\langle p\rangle}{dx}, \qquad (24)$$

where Rem. stands for the remaining terms in Eq. (18) and includes the rate of change (increase) of $\widetilde{u''^2}$ with time (expected to be zero at steady state) and the rate of change of $\widetilde{u''^2}$ due to the reorientation term (expected to be small). Thus the remainder term is expected to be nearly zero throughout the flame. On the other hand, if the remainder term is large in comparison with the other terms in Eq. (24), it can be inferred that the "slow" pressure plays an important role (Rem. is identically zero in the BML study [7]). The terms on the right-hand side of Eq. (24) are, in order from left to right, due to convection, turbulent diffusion, dilatation, and mean pressure gradient. All the terms in Eq. (24) are zero for $R = 1$.

Figure 8 shows the terms in Eq. (24) as a function of $\tilde{c}$ for density ratios of 8.0 (Fig. 8a) and 2.0 (Fig. 8b) and in the BML study [7] ($R = 7.5$, Fig. 8c). The figures show that the balance of $\widetilde{u''^2}$ is dominated by convection, dilatation and mean pressure gradient terms, and turbulent diffusion plays a minor role. It is seen that the dilatation

Fig. 8a.

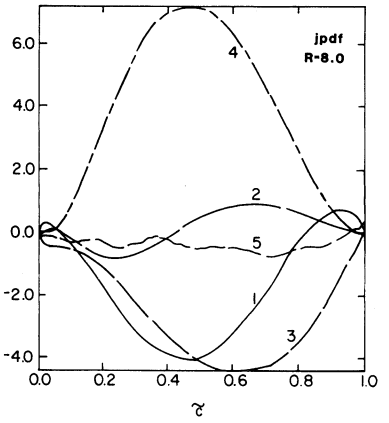

Fig. 8b.

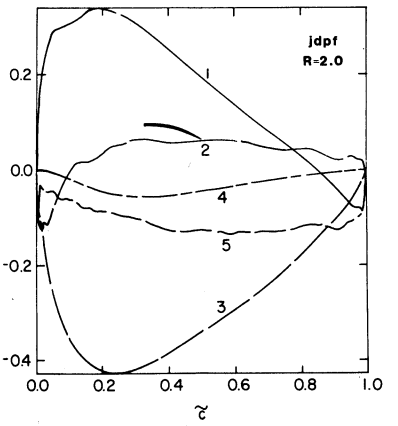

Fig. 8c.

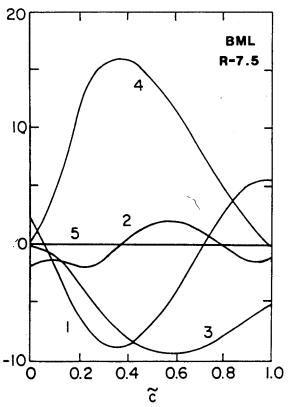

Fig. 8. Balance of terms in the equation for the streamwise velocity variance [Eq. (24)]: (a) present study, $R = 8.0$; (b) present study, $R = 2.0$; (c) BML theory, $R = 7.5$ (Libby [7]). Key: 1 = convection $(-\langle\rho\rangle\tilde{u}d\widetilde{u''^2}/dx)$; 2 = turbulent diffusion $(-d\langle\rho\rangle\widetilde{u''^3}/dx)$; 3 = destruction (dilation) $(-2\langle\rho\rangle\widetilde{u''^2}d\tilde{u}/dx)$; 4 = production (mean pr. grad.) $(-2\langle u''\rangle d\langle p\rangle/dx)$; 5 = remainder (1 + 2 + 3 + 4).

term is destructive (i.e., a sink) for all density ratios and its magnitude decreases with decreasing R. The mean pressure gradient term $(-2\langle u''\rangle d\langle p\rangle/dx)$ is a production term for large density ratios (say $R \geq 4$) ($\langle u''\rangle$ is positive—see Eq. (20) and Fig. 7a—and $d\langle p\rangle/dx$ is negative). The magnitude of the mean pressure gradient term decreases with decreasing R since both $\langle u''\rangle$ and the absolute value of $d\langle p\rangle/dx$ decrease, until the term becomes a sink (Fig. 8b). This is due to the change in sign of $\langle u''\rangle$ (rather, of $\widetilde{u''c''}$) for $R < 2.5$ (inferred from Fig. 7a and Ref. [13]). The change in sign of $\widetilde{u''c''}$ is, again, attributable to the small values of $d\langle p\rangle/dx$ at low density ratios as discussed before. For $R = 8.0$ (Fig. 8a) the production due to mean pressure gradient dominates the destruction due to dilatation up to approximately $\tilde{c} = 0.7$, beyond which the effect of dilatation dominates the effect of the mean pressure gradient. Hence, the variance $\widetilde{u''^2}$ is expected to increase in the initial part of the flame and decrease in the later part of the flame, thus peaking within the flame. The variation of the convection term (Fig. 8a) indicates that $\widetilde{u''^2}$ peaks near $\tilde{c} = 0.8$. On the other hand, for $R = 2.0$ (Fig. 8b), both the dilatation and the mean pressure gradient terms are destructive, and $\widetilde{u''^2}$ is expected to decrease continuously through the flame, except for the effect of the reorientation term (Rem.) which may cause a slight increase in $\widetilde{u''^2}$ beyond $\tilde{c} = 0.85$. This trend is indeed indicated by the convection term in Fig. 8b. It is interesting to note that the profiles of the various terms in Eq. (24) remain nearly unchanged (though their magnitudes change) for all $R \geq 6$ [13].

The terms in Eq. (24) *as obtained* from the BML theory [7] are shown in Fig. 8c for $R = 7.5$. The terms shown in Fig. 8c have to be multiplied by $d\tilde{c}/dx$ at each $\tilde{c}$ in order to correspond to the terms in Eq. (24)—$d\tilde{c}/dx$ is unknown in the BML theory. Therefore, a quantitative comparison with the present results (Fig. 8a) is not possible. However, a comparison of Figs. 8a and 8c (which are for approximately the same density ratio) shows that the profiles of the various terms are very similar in the two studies.

The profiles of the streamwise velocity variance $\widetilde{u''^2}$ normalized by the upstream variance are shown for different density ratios in Fig. 9 with the results from the present study in Fig. 9a and those from the BML theory [6] in Fig. 9b. The trends seen in Fig. 9 bear out the discussion with regard to the balance of terms in Eq. (24). Results from both of the studies show a significant increase in $\widetilde{u''^2}$ through the flame for $R \geq 6$. The variance peaks within the flame for $R \geq 6$, and the location of the peak is nearly independent of the density ratio in both the studies—near $\tilde{c} = 0.8$ in the present study (Fig. 9a) and near $\tilde{c} = 0.75$ in the BML study (Fig. 9b). This result is consistent

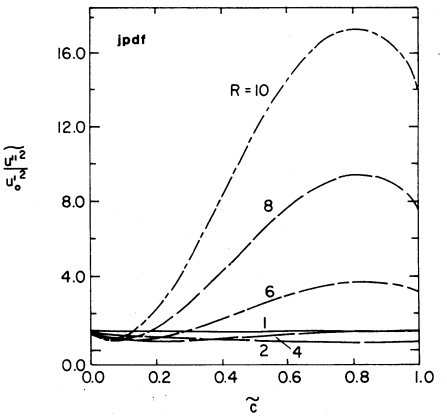

Fig. 9a.

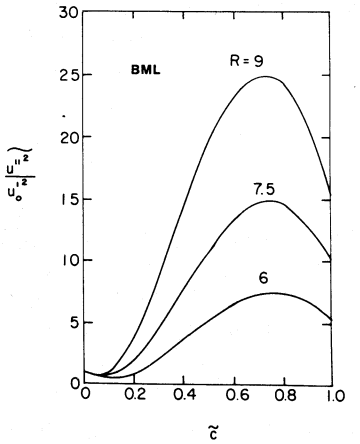

Fig. 9b.

Fig. 9. Streamwise velocity variance (normalized by the upstream variance) against mean progress variables with density ratio as a parameter: (a) present study; (b) BML theory (Bray et al. [6]).

with the observation that the profiles of the balance terms [Eq. (24)] are identical in shape for $R \geq 6$ [13]. Results from both studies (Fig. 9) show an initial region near the cold boundary where the variance decreases from its upstream value before increasing again for $R \geq 4$. The extent of this region depends on the value of R. The larger the value of R, the smaller the region. The initial decrease in $\widetilde{u''^2}$ is due to the fact that the destructive dilatation term is nonzero while the production term due to mean pressure gradient is nearly zero in that region (Figs. 8a and 8b).

A comparison of the results in Fig. 9a and Fig. 9b shows that the variance calculated in the BML study is significantly higher than in the present study. Again, it can be argued that this difference is due to the different values of S_T in the two studies. A study of the sensitivity of the BML calculations to the value of S_T [7] showed that an increase in S_T/u_0' from 2.1 to 2.5 increased the value of $\widetilde{u''^2}$ by nearly 50% for $R = 6$. The reason for this sensitivity is that the mean pressure gradient, which plays a major role in the production of the variance, is a strong function (quadratic) of the flame speed. A higher value of S_T leads to a higher production as well as a higher sink term (increase in the diltation term). But the increase in the production term is greater than the increase in the dilatation term [13].

Figure 10 shows the unconditional and conditional third moments, normalized by $u_0'^3$, for $R =$ 8.0 from the present study. The figure shows that the unconditional streamwise velocity distribution within the flame is highly skewed. The skewness $(=\widetilde{u''^3}/(\widetilde{u''^2})^{3/2})$ is 0.27 at $\tilde{c} = 0.4$. In addition, it is seen that the conditional third moments are comparable in magnitude to the unconditional third moment, and are not negligible as assumed in the BML theory. The skewness in the burned and unburned velocity distributions $(\langle u'^3\rangle_b/\langle u'^2\rangle_b^{3/2}$ and $\langle u'^3\rangle_u/\langle u'^2\rangle_u^{3/2})$ are -0.23 and 0.95, respectively, at $\tilde{c} = 0.6$, and are -0.24 and 0.69, respectively at $\tilde{c} = 0.8$. [It should be noted that conditional averages are ill-conditioned in certain regions of the flame, namely, the burned averages at the cold edge of the flame (near $\tilde{c} = 0$) and the unburned averages at the product edge (near $\tilde{c} = 1$). As a result, the determination of these quantities is subject to large statistical errors in such regions. The wiggles in the profile of $\langle u'^3\rangle_u$ seen in Fig. 10 can be attributed to this fact.]

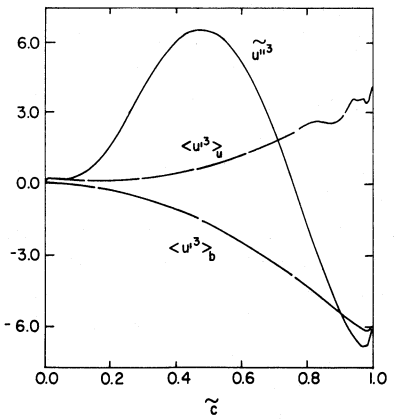

Fig. 10. Unconditional and conditional third moments of velocity as functions of the mean progress variable for $R =$ 8.0. The third moments are normalized by $u_0'^3$.

The results presented here in conjunction with additional results [13], including those for transverse velocity variances, show that the turbulence continues to evolve in the product stream (beyond the physical location where $\tilde{c} = 1$ is reached), suggesting that the turbulence ultimately becomes isotropic and nonskewed far downstream of the flame. This result is to be expected since, with the absence of effects other than viscous dissipation and the balancing energy addition in the fully burned gas, the effect of the reorientation term is to make the velocity distribution joint-normal.

The models used in the BML theory are now evaluated against the results from the present study. Specifically, the BML models for $(\langle u'^2\rangle_b - \langle u'^2\rangle_u)$ and the conditional third moments are investigated.

Figure 11 shows the BML model [7] for the difference between the conditional variances compared with the results calculated from the mdf in the present study. The figure shows a significant discrepancy between the present results and the BML model both qualitatively and quantitatively—the BML model assumes a linear variation with $\tilde{c}$. Bray et al. [6] and Libby [7] report that the overall predictions for the flame are insensitive to the modeling of the conditional variances, although it is apparent from their studies that the magnitude of

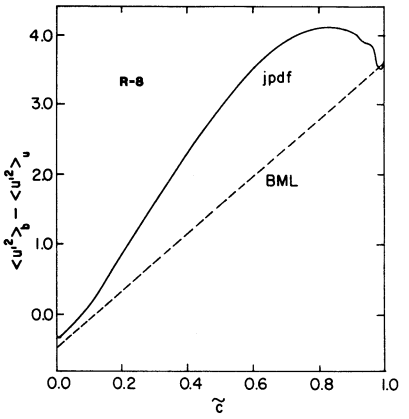

Fig. 11. Comparison of the BML model (Libby [7]) for the conditional variances against results from the present study, $R = 8.0$. The variances are normalized by the upstream variance.

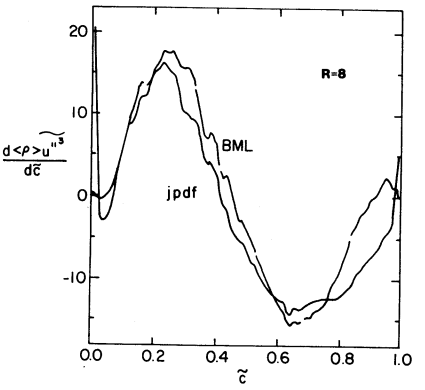

Fig. 12. Comparison of the diffusion term in the balance equation for the streamwise velocity variance [Eq. (24)] between results in the present study and that calculated based on the BML assumptions regarding conditional third moments.

the unconditional streamwise variance is affected by the modeling. Also, results presented in Ref. [13] show that the burned variance makes a significant contribution to the unconditional variance in the region where $\tilde{c}$ is greater than 0.6, a region where the maximum discrepancy between the BML model and the present results exists. In particular, the peak value of the variance (occurring near $\tilde{c} = 0.8$) is affected by the modeling.

The results presented in Fig. 10 show that the assumption in the BML theory that the conditional third moments are zero may not be justified. The conditional third moments make a significant contribution to the unconditional third moment especially beyond $\tilde{c} = 0.6$ [13]. It is expected that the effect of this modeling on the equations solved in the BML theory (see previous section) is felt only through the diffusion term $d\langle\rho\rangle\widetilde{u''^3}/dx$ in Eq. (24), or more precisely through the term $d\langle\rho\rangle\widetilde{u''^3}/d\tilde{c}$. The term is shown in Fig. 12 as calculated from the mdf in the present study as well as from Eq. (22) with the BML assumption for the conditional third moments. The figure shows that both calculations yield nearly the same value for the term through the bulk of the flame except for the small difference near the product edge of the flame ($\tilde{c} > 0.8$). This difference is not likely to affect the calculations of the flame since the contribution of the diffusion term to the balance equation [Eq. (24)] is not significant (see Fig. 8).

The computer resource required for the present study was quite modest. The computations were performed either on a VAX 11/750 or an equivalent Masscomp machine. The CPU time required for each run was approximately 13 h. This CPU time is equivalent to approximately 20 min on an IBM 3081.

CONCLUSIONS

Idealized premixed turbulent flames have been studied using pdf methods. A modeled transport equation for the joint pdf of velocity and the progress variable has been solved by a Monte Carlo method. The effects of variable-density on flame properties as well as the competing mechanisms within the flame have been studied. The results have been compared with available experimental data [14] and the results from the BML (Bray–Moss–Libby) theory [6, 7]. The models used in the BML theory have been evaluated against the present calculations.

It is seen that the turbulent flame speed S_T attains an asymptotic value of approximately $1.5u_0'$ and is nearly independent of the density ratio (R) for $R > 4$, while the turbulent flame thickness increases almost linearly with R. The profile of variation of the mean progress variable is universal and independent of R in a coordinate system nondimensionalized by the flame thickness.

It is seen that the mean pressure gradient plays a very important role in the production of turbulence and scalar flux within the flame. The magnitude of the mean pressure gradient increases with increasing R. The other important terms in the balance equations for turbulent kinetic energy and the scalar flux are the convection (by mean velocity) and dilatation (volume expansion) terms. The effect of the pressure fluctuations due to turbulence alone is small.

The results are in good agreement with the available experimental data and the results from the BML theory for premixed turbulent flames. A value ($=2.1u_0'$) is assumed for the turbulent flame speed in the BML theory. The quantitative differences between the results from the present study and those from the BML theory can be attributed to the difference between the value of S_T calculated in the present study and that assumed in the BML theory.

The present pdf approach has certain advantages over the BML approach. Fewer models are required in the present approach than in the BML theory—important processes such as convection, reaction, and the effect of the mean pressure gradient appear in closed form in the present approach. Flame speed and the structure of the flame are calculated in the present study, while the former is assumed and the latter is unknown in the BML theory.

The results from the present study show that the BML models for the conditional variances and third moments may be inaccurate. The model for the conditional third moments may not significantly affect the results, while the model for the conditional variances can affect the peak value of the unconditional variance within the flame.

The treatment, including the neglect, of terms involving pressure fluctations is a major source of uncertainty in the present study as well as in the BML studies. The importance of the pressure fluctuations due to variable-density effects needs to be investigated both experimentally and theoretically, and suitable models need to be developed. In addition, the present approach should be applied to multidimensional and more easily realizable laboratory flames so that the computed results and experimental data can be directly compared. These comparisons will be instrumental in the review of current models and will also provide guidance to future modeling efforts.

ACKNOWLEDGMENT

This work was performed at Cornell University during the course of the first author's doctoral dissertation, and was supported by Grant No. DAAG29-84-K-0020 from the U.S. Army Research Office.

REFERENCES

1. Libby, P. A., and Williams, F. A. (Eds.), *Turbulent Reacting Flows* (Topics in Applied Physics 44), Springer-Verlag, 1980.
2. Pope, S. B., *Progress in Energy and Combustion Science* 11:119–192 (1985).
3. Heywood, J. B., *Progress in Energy and Combustion Science* 1:135 (1976).
4. Keck, J. C., *Nineteenth Symposium (International) on Combustion,* The Combustion Institute, Pittsburgh, 1982, pp. 1451–1466.
5. Stambuleanu, A., *Flame Combustion Processes in Industry,* Abacus, Tunbridge Wells, England, 1976.
6. Bray, K. N. C., Libby, P. A., Masuya, G., and Moss, J. B., *Combustion Science and Technology* 25:127–140 (1981).
7. Libby, P. A., *Progress in Energy and Combustion Science* 11:83–96 (1985).
8. Pope, S. B., and Anand, M. S., *Twentieth Symposium (International) on Combustion,* The Combustion Institute, Pittsburgh, 1984, pp. 403–410.
9. Bray, K. N. C., and Moss, J. B., *Acta Astronautica* 4:291–319 (1977).
10. Pope, S. B., *Physics of Fluids* 24:588–596 (1981).
11. Pope, S. B., *Combustion Science and Technology* 28:131–145 (1982).
12. Pope, S. B., in *Turbulent Shear Flows 3* (L. J. S. Bradbury et al., Eds.), Springer-Verlag, Berlin, Heidelberg, 1982.
13. Anand, M. S., Ph.D. Thesis, Cornell University, Ithaca, NY, 1986.
14. Moss, J. B., in *Combustion Science and Technology* 22:119–129 (1980).
15. Pope, S. B., *Philosophical Transactions of The Royal Society of London* A291:529–568 (1979).
16. Bray, K. N. C., Libby, P. A., and Moss, J. B., *Combustion Science and Technology* 41:143–172 (1984).
17. Namazian, M., Talbot, L., and Robben, F., *Twentieth*

Symposium (International) on Combustion, The Combustion Institute, Pittsburgh, 1984, pp. 411–419.
18. Rotta, J. C., *Zeitschrift fur Physik* 129:547–572 (1951).
19. Launder, B. E., Reece, G. J., and Rodi, W., *Journal of Fluid Mechanics* 68:537–566 (1975).
20. Anand, M. S., and Pope, S. B., *Turbulent Shear Flows 4* (L. J. S. Bradbury et al., Eds.), Springer-Verlag, Berlin, Heidelberg, 1985.
21. Gosman, A. D., Private communication, Imperial College, London, 1985.
22. Hackberg, B., and Gosman, A. D., *Twentieth Symposium (International) on Combustion,* The Combustion Institute, Pittsburgh, 1984. pp. 225–232.
23. Bray, K. N. C., and Libby, P. A., *Physics of Fluids* 19:1687–1701 (1976).
24. Libby, P. A., and Bray, K. N. C., *AIAA Journal* 19:205–213 (1981).

Received 27 June 1986; revised 11 September 1986